Available online at www.sciencedirect.com

SCIENCE DIRECT®

Global and Planetary Change 45 (2005) 207–236

GLOBAL AND PLANETARY CHANGE

www.elsevier.com/locate/gloplacha

Magnetostratigraphic chronology of a late Eocene to early Miocene glacimarine succession from the Victoria Land Basin, Ross Sea, Antarctica

Fabio Florindo[a,*], Gary S. Wilson[b], Andrew P. Roberts[c], Leonardo Sagnotti[a], Kenneth L. Verosub[d]

[a]*Istituto Nazionale di Geofisica e Vulcanologia, Via di Vigna Murata, 605, I-00143 Rome, Italy*
[b]*Department of Geology, University of Otago, P.O. Box 56, Dunedin, New Zealand*
[c]*School of Ocean and Earth Science, University of Southampton, Southampton Oceanography Centre, European Way, Southampton SO14 3ZH, U.K.*
[d]*Department of Geology, University of California, Davis, CA 95616, U.S.A.*

Accepted 28 September 2004

Abstract

Drilling offshore from Cape Roberts, Antarctica, has enabled recovery of a 1472-m cumulative record of late Eocene–early Miocene history of sedimentary basin development and climate change in the Western Ross Sea. In this paper, we synthesize the results of palaeomagnetic analyses carried out on the CRP-1, CRP-2 and CRP-3 sediment cores, and present a chronology for the recovered Eocene–Miocene succession. Stepwise demagnetization data demonstrate that secondary overprints have been successfully removed and that characteristic remanent magnetizations (ChRMs) have been clearly identified in most of the samples. A close sampling interval has allowed a detailed magnetic polarity stratigraphy to be established for the composite succession. Correlation with the geomagnetic polarity time scale (GPTS) has been constrained by a number of $^{40}Ar/^{39}Ar$ and $^{87}Sr/^{86}Sr$ ages, as well as by a recently developed Antarctic siliceous microfossil zonation, and by calcareous nannoplankton biostratigraphy. The basal sediments of the Eocene–Miocene succession rest unconformably on Devonian sandstones of the Beacon Supergroup. A basal sandstone breccia, which probably represents the onset of rifting in the Victoria Land Basin (VLB), is overlain by a succession of sandstones that are interbedded with thin conglomerate beds. These sediments give way to more clearly glacially influenced mudstones and diamictite facies in the mid Oligocene, and, by the Oligocene–Miocene boundary, coincident with the Mi-1 glaciation, a permanent glacial dominance was imprinted on the sedimentary record. Average sediment accumulation rates were initially rapid in the late Eocene–early Oligocene (up to 60 cm/k.y.), but reduced to only a few cm/k.y. in the early Miocene as basin subsidence slowed.

Keywords: Antarctica; Cape Roberts Project; Cenozoic; Chronology; Magnetostratigraphy

* Corresponding author. Tel.: +39 0651860383; fax: +39 0651860397.
E-mail address: florindo@ingv.it (F. Florindo).

0921-8181/$ - see front matter © 2004 Elsevier B.V. All rights reserved.
doi:10.1016/j.gloplacha.2004.09.009

1. Introduction

In the early 1990s, a multinational group (Australia, Germany, Italy, New Zealand, the Netherlands, U.K., and U.S.A.) was established with the aim of obtaining a continuous stratigraphic record from beneath western McMurdo Sound by drilling three overlapping drill-holes through a dipping sedimentary succession that intersects the sea floor at Roberts Ridge, as part of the Cape Roberts Project (henceforth CRP; Cape Roberts Science Team, 1998, 1999, 2000; Hambrey et al., 1998; Barrett et al., 2000, 2001; Davey et al., 2001). The project was named after Cape Roberts, a small promontory 125 km northwest of McMurdo Station (U.S.) and Scott Base (N.Z.), which was the staging point for the offshore drilling (Fig. 1). The purpose of the CRP was to: (1) establish the chronology of events associated with the onset and subsequent history of Antarctic continental glaciation, and (2) date the onset of rifting in the West Antarctic Rift System and uplift of the Transantarctic Mountains (TAM) which represent the associated rift shoulder (Barrett and Davey, 1992; Webb and Wilson, 1995; Davey et al., 2001). The three holes were drilled, from a sea-ice platform, along a transect and were spaced in order to recover progressively older strata by penetrating seaward-dipping seismic reflectors (Hamilton et al., 2001; Henrys et al., 2001; Figs. 1 and 2).

Cape Roberts lies in the southwestern corner of the Ross Sea between the TAM in southern Victoria Land and Ross Island, at the southern end of the Victoria Land Basin (VLB), which is the westernmost of four north-south-trending rift basins that comprise the West Antarctic Rift System (Davey et al., 1982, 1983; Cooper et al., 1987; Fig. 1). The VLB contains up to 14 km of seaward-dipping Mesozoic–Cenozoic strata (Cooper et al., 1987; Brancolini et al., 1995). Two main crustal thinning events are thought to have produced the basins of the West Antarctic Rift System (Houtz and Davey, 1973; Cooper et al., 1987), but their age is not well constrained. The first event was a phase of nonmagmatic extension across the whole of the Ross Sea associated with the late Mesozoic (pre-80 Ma?) break-up of Gondwana. The second event, which was largely confined to the VLB, began in the late Eocene–early Oligocene (Cape Roberts Science Team, 1999, 2000) and is thought to have been linked to the early uplift of the TAM (Fitzgerald, 1992). This second event also resulted in rift-related volcanism, which continues to be active today (e.g., the volcanoes of Ross Island).

The TAM provide the dominant source of sediment for the VLB. The TAM succession comprises granitic and metamorphic basement (Gunn and Warren, 1962), which is separated from the overlying flat-lying Devonian to Triassic continental sediments of the Beacon Supergroup by an unconformity known as the Kukri erosion surface (Barrett, 1981). The Beacon Supergroup is extensively intruded by the Jurassic Ferrar Supergroup (Harrington, 1958). The only Cenozoic rocks known to crop out in the TAM are exposures of pre-Quaternary glacigene sediments, known as the Sirius Group (e.g., Mercer, 1968; Mayewski, 1975; McKelvey et al., 1991), and Miocene–Pliocene basaltic cinder cones of the McMurdo Volcanic Group (e.g., Armstrong, 1978; Kyle, 1990; Wilch et al., 1993).

1.1. The CRP succession

The basement of the VLB was penetrated at 823 mbsf in the CRP-3 drill-hole and a further 133 m of recovered basement rocks have been correlated with the Devonian Arena Sandstone of the Beacon Supergroup (Cape Roberts Science Team, 2000) (Fig. 3). The basement rocks are unconformably overlain by ~500 m of coarse-grained siliciclastic sediments that are interpreted to represent an early rift succession that was deposited during inception of the VLB. This succession includes a 30-m-thick late Eocene–early Oligocene basal sandstone breccia (Hannah et al., 2001a,b) that is overlain by more than 400 m (up to ~300 mbsf in the CRP-3 drill-hole) of sandstones with subordinate conglomerates. Above ~300 mbsf in the CRP-3 drill-hole, and through the lower ~300 m of the CRP-2 drill-hole, the succession fines and progressively becomes more obviously glacially dominated with increasing occurrences of mudstone and diamict facies. The succession also becomes more clearly cyclic in nature, with a particularly thick series of cycles encompassing the Oligocene–Miocene Boundary (Naish et al., 2001). Early Miocene glacial sediment persists above the Oligocene–Miocene boundary until it is truncated by a major unconformity at 26.79 mbsf in the CRP-2 drill-hole (43.55 mbsf in

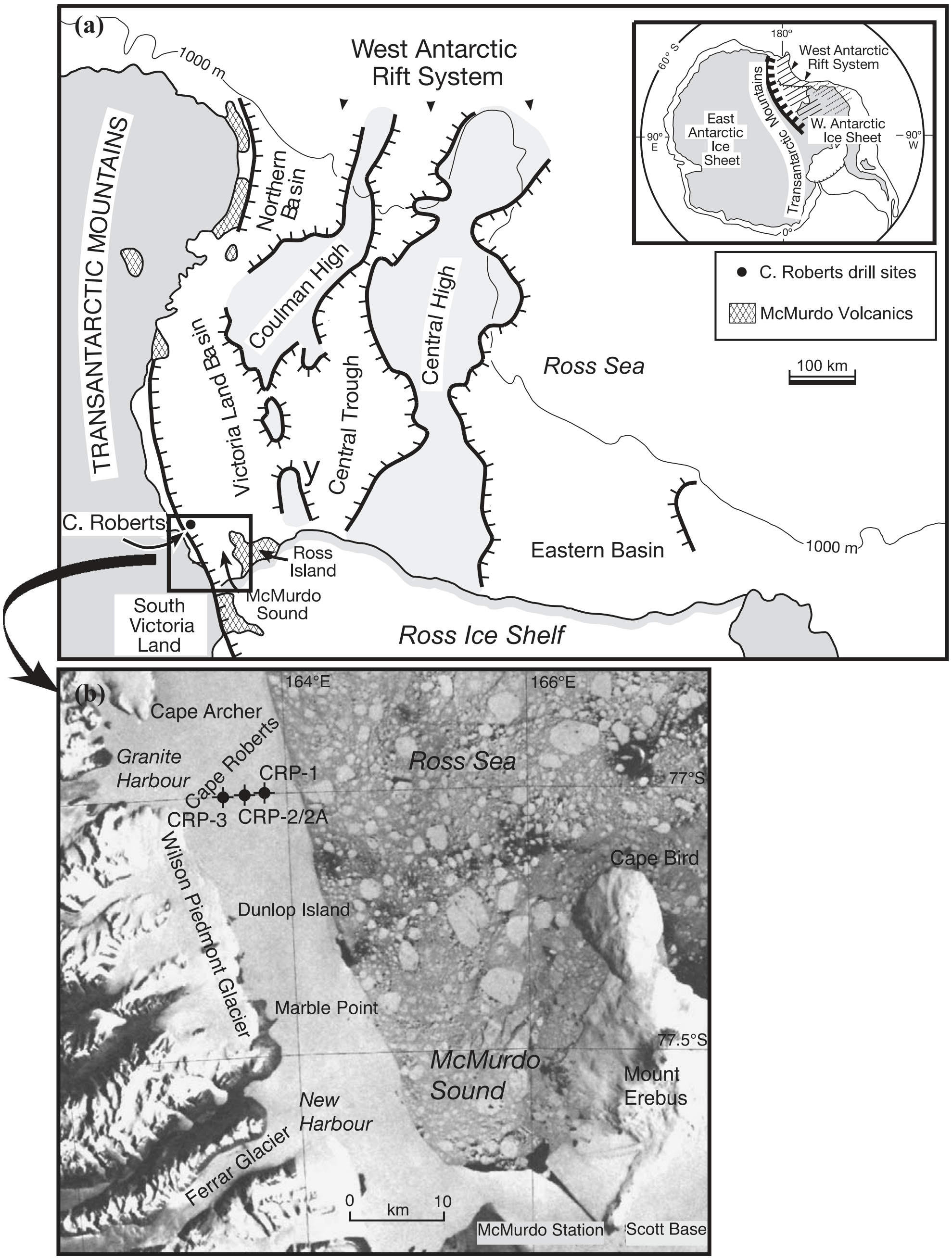

Fig. 1. (a) Location map of the Victoria Land Basin with respect to the West Antarctic rift system (inset). Thick black lines represent inferred basin margins and tick marks represent the down-thrown side on possible basement fault blocks. (b) Satellite image of the southwestern Ross Sea, with the location of the CRP drill-holes. The box on the location map indicates the location of the satellite image.

the CRP-1 drill-hole), above which sandy Quaternary glacial sediments were recovered (Cape Roberts Science Team, 2000).

In this paper, we synthesize the results of our palaeomagnetic analyses of the CRP-1, CRP-2, and CRP-3 sediment cores (Roberts et al., 1998; Wilson et

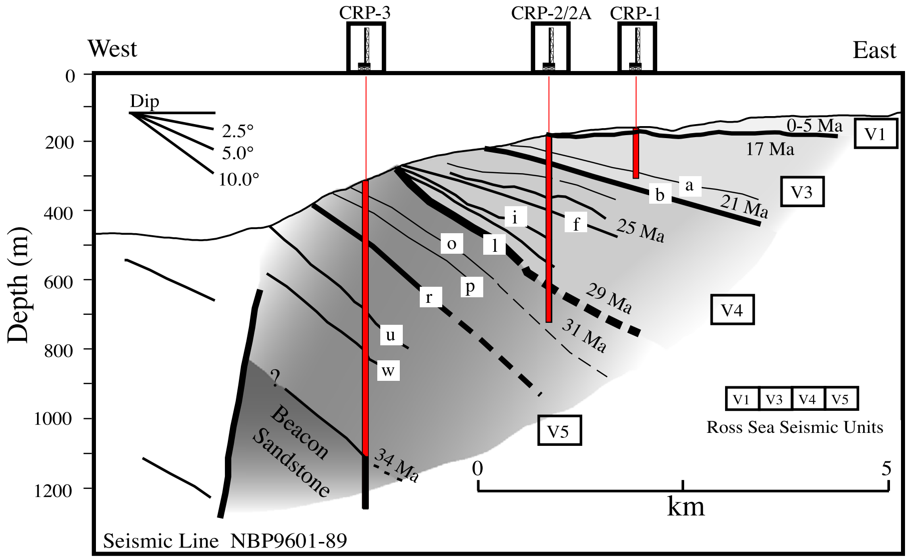

Fig. 2. Geological cross-section based on single channel seismic line NBP9601-89, from offshore of Cape Roberts, showing the configuration of seaward-dipping reflectors sampled in the CRP-1, CRP-2, and CRP-3 drill-holes, after Hamilton et al. (2001) and Henrys et al. (2001).

al., 2000a,b; Florindo et al., 2001), and present an integrated chronology for the Eocene–Miocene succession recovered from these drill sites. Our chronology allows comparison with lower latitude records and allows rates and modes of sedimentation to be established for the western margin of the Victoria Land Basin (VLB) in close proximity to the TAM and East Antarctic craton.

2. Methods

2.1. Sampling

Thick intervals of the CRP succession comprise coarse-grained lithologies (Fig. 3), which would not normally be considered to be well suited to palaeomagnetic investigations because they are more likely to contain coarse magnetic particles that are incapable of carrying a long-term palaeomagnetic record. However, the diamictites in the CRP succession contain a significant silt-sized component that has proven to be suitable for palaeomagnetic analysis. It has been, therefore, possible to develop polarity records for even the coarsest sedimentary units in the CRP succession.

Where possible, samples were collected from fine-grained horizons at 0.5-m spacing; intervals with obvious drilling-related deformation were not sampled. A total of 2189 oriented discrete samples were collected from the centre of the working half of the Eocene–Miocene succession recovered in the CRP-1, CRP-2, and CRP-3 cores. One hundred and fifty pairs of samples (separated stratigraphically by a few centimetres) were taken from varying lithofacies at regular intervals throughout the succession for a pilot study that was aimed at assessing the most suitable demagnetization technique for routine treatment of the remaining samples.

Unconsolidated sediments were sampled with standard 6 cm^3 plastic boxes (151 samples) and consolidated sediments were sampled by drilling conventional cylindrical (25 mm diameter×22 mm height) palaeomagnetic samples (2038 samples) using a modified drill press. The samples were oriented with respect to vertical and with respect to a vertical core-recovery reference scribe-line. The scribe-line was not always continuous across core breaks; therefore, it was not possible to orient the samples azimuthally. Lack of azimuthal orientation of the samples did not pose a problem for polarity determination because the geomagnetic field at the latitude of the drill-sites

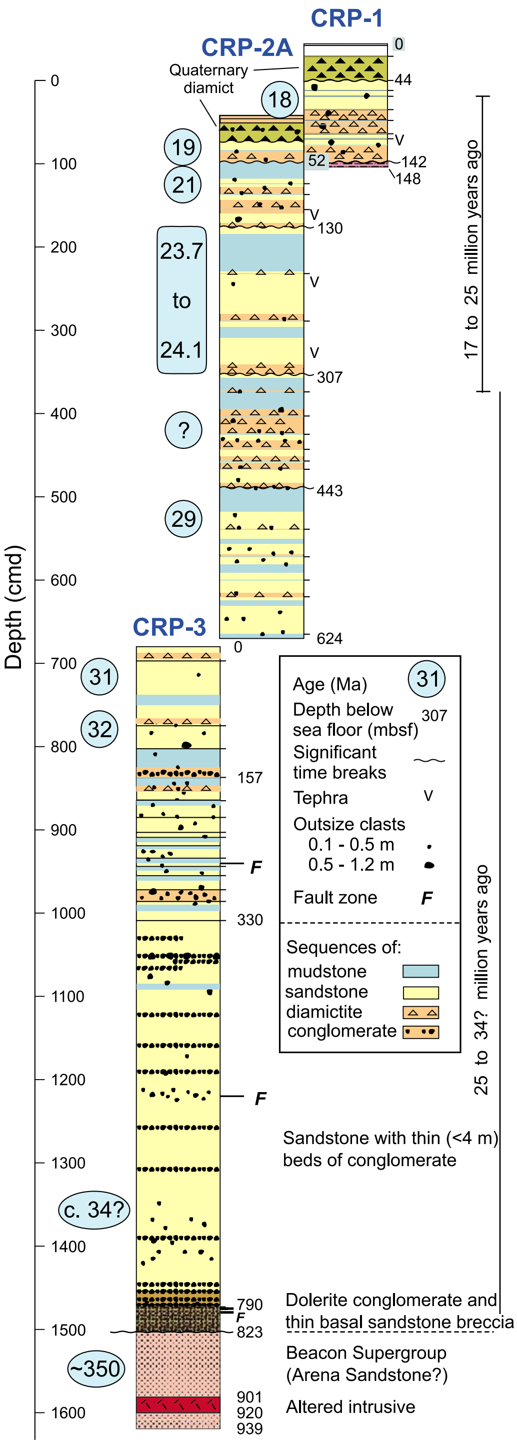

Fig. 3. Composite lithostratigraphic log for the CRP-1, CRP-2, and CRP-3 drill-cores (modified from Barrett et al., 2001). Ages are from the composite age models discussed in the text. Calculation of the cumulative metres drilled is shown in Table 1.

(77°S) has a steep inclination (83.4° assuming a geocentric axial dipole field).

2.2. Pilot studies

Before performing routine demagnetization of all samples from the CRP cores, pilot studies were conducted at McMurdo Station (using an AGICO JR-5A spinner magnetometer; Florindo et al., 1997; Cape Roberts Science Team, 1998, 1999, 2000) to determine the most appropriate demagnetization technique for isolating the characteristic remanent magnetization (ChRM). One sample from each of the 150 pairs of pilot samples was subjected to alternating field (AF) demagnetization at successive peak fields of 5, 10, 15, 20, 25, 30, 40, and 50 mT; for some samples, some of the following steps were added: 35, 45, 60, 70, 80, 90, and 100 mT. The remaining samples were subjected to progressive thermal demagnetization from room temperature up to 650 °C in 40° increments from 80 to 600 °C for samples from CRP-1 and at steps of 120, 180, 240, 300, 350, 400, 450, 500, 550, 600, and 650 °C for samples from CRP-2 and CRP-3. The low-field magnetic susceptibility (κ) was monitored after each heating step (using a Bartington Instruments magnetic susceptibility meter with MS-2B probe) in order to detect any thermally induced changes in the magnetic mineralogy. Further heating was abandoned if a susceptibility increase of more than 30% was observed, with a concomitant loss of coherence in the palaeomagnetic signal.

2.3. Measurements

Pilot studies demonstrated that thermal and AF demagnetization were equally effective in removing secondary remanence components and in isolating the ChRM. Therefore, AF demagnetization, up to peak fields of either 60 or 70 mT, was adopted for routine treatment of samples because it was less time-consuming and because it avoided the possibility of thermal alteration during demagnetization. Time constraints or the friable or fractured nature of samples limited the number of specimens that could be measured on the JR-5A high-speed spinner magnetometer that was housed temporarily at McMurdo Station during the three drilling seasons (Florindo et al., 1997). Of the 2189 samples collected (including the 300 pilot samples), 979 (39%) were subjected to complete palaeomagnetic analysis at McMurdo Station. The remaining samples were transported to the respective palaeomagnetic laboratories at the Istituto Nazionale di Geofisica e Vulcanologia, Rome (INGV), and the University of California, Davis (UCD), for AF demagnetization. In both laboratories, samples were analysed within a magnetically shielded room using a 2-G Enterprises automated, pass-through cryogenic magnetometer with in-line AF demagnetization capability.

During the drilling seasons, κ was measured for all samples. Following the drilling season, additional rock magnetic studies were carried out at the INGV, UCD, at the Southampton Oceanography Centre (SOC) and at the University of Oxford, on AF-demagnetized samples or on chips or powders collected during sampling. Analyses included acquisition of an anhysteretic remanent magnetization (ARM) in a peak field of 100 mT with a superimposed 0.1 mT bias field, stepwise acquisition of an isothermal remanent magnetization (IRM) up to 1 T and back-field demagnetization of the IRM up to -0.3 T with determination of coercivity of remanence (B_{cr}) and the S-ratio ($-IRM_{-300\ mT}/IRM_{1\ T}$), thermomagnetic, and hysteresis measurements (including measurement of the saturation remanence, M_{rs}; saturation magnetization, M_s; B_{cr}; and coercive force, B_c). ARMs and IRMs were subsequently stepwise demagnetized up to 100 mT, using the in-line system on the 2-G Enterprises cryogenic magnetometer at the INGV. Hysteresis loops were measured using a Princeton Measurements Micromag alternating gradient magnetometer (maximum field of 1.4 T) at UCD. Thermomagnetic analyses were conducted at the SOC using a variable field translation balance, with a field of 76 mT and a heating rate of 10 °C/min in air, and at the University of Oxford using an AGICO KLY-2 Kappabridge magnetic susceptibility meter coupled with a CS-2 furnace.

Rock magnetic data are discussed here only if they are necessary to understand the mineralogical carriers of the palaeomagnetic signal. More detailed presentation of the magnetic properties is given elsewhere (Roberts et al., 1998; Sagnotti et al., 1998, 2001 Verosub et al., 2000; Wilson et al., 2000a,b; Florindo et al., 2001).

3. Results—rock magnetic properties

3.1. CRP-1 drill-core

Throughout the CRP-1 succession, down-core variations of κ are associated with similar changes in all of the investigated concentration-dependent magnetic parameters (Sagnotti et al., 1998; Roberts et al., 1998; Fig. 4). In particular, high concentrations of ferrimagnetic minerals occur in two main intervals (from 92.2 to 105.8 mbsf and from 124.2 to 143.8 mbsf). Unambiguous evidence concerning magnetic mineralogy was obtained only from these high κ intervals. In each case, the thermomagnetic behaviour is clearly consistent with that of magnetite (Sagnotti et al., 1998; Roberts et al., 1998). Hysteresis data are typical of pseudo-single domain (PSD) magnetite (cf. Day et al., 1977) except for the lowermost 4.5 m of the core, where hysteresis parameters suggested the presence of the ferrimagnetic iron sulphide mineral, greigite (Fe_3S_4; cf. Roberts, 1995). Roberts et al. (1998) observed a complex polarity pattern in the lowermost 4.5 m of the CRP-1 core, where 18 apparent polarity reversals are recorded. This alternation of polarities coincides with an alternation in magnetic properties, with reversed polarity intervals dominated by magnetite and normal polarity intervals apparently dominated by greigite. Roberts et al. (1998) concluded that this mixed polarity interval with alternating magnetic properties was probably remagnetized and did not interpret the apparent magnetostratigraphy from this interval. Subsequent detailed scanning electron microscope observations of polished sections from this interval (Sagnotti et al., 2005) confirm that greigite is present and that it occurs in alternating bands, in intimate association with patches of authigenic siderite cement (Baker and Fielding, 1998; Claps and Aghib, 1998). Sedimentary microtextures indicate that the greigite formed on the surfaces of the authigenic siderite grains. We therefore interpret the observed remagnetization of the lower

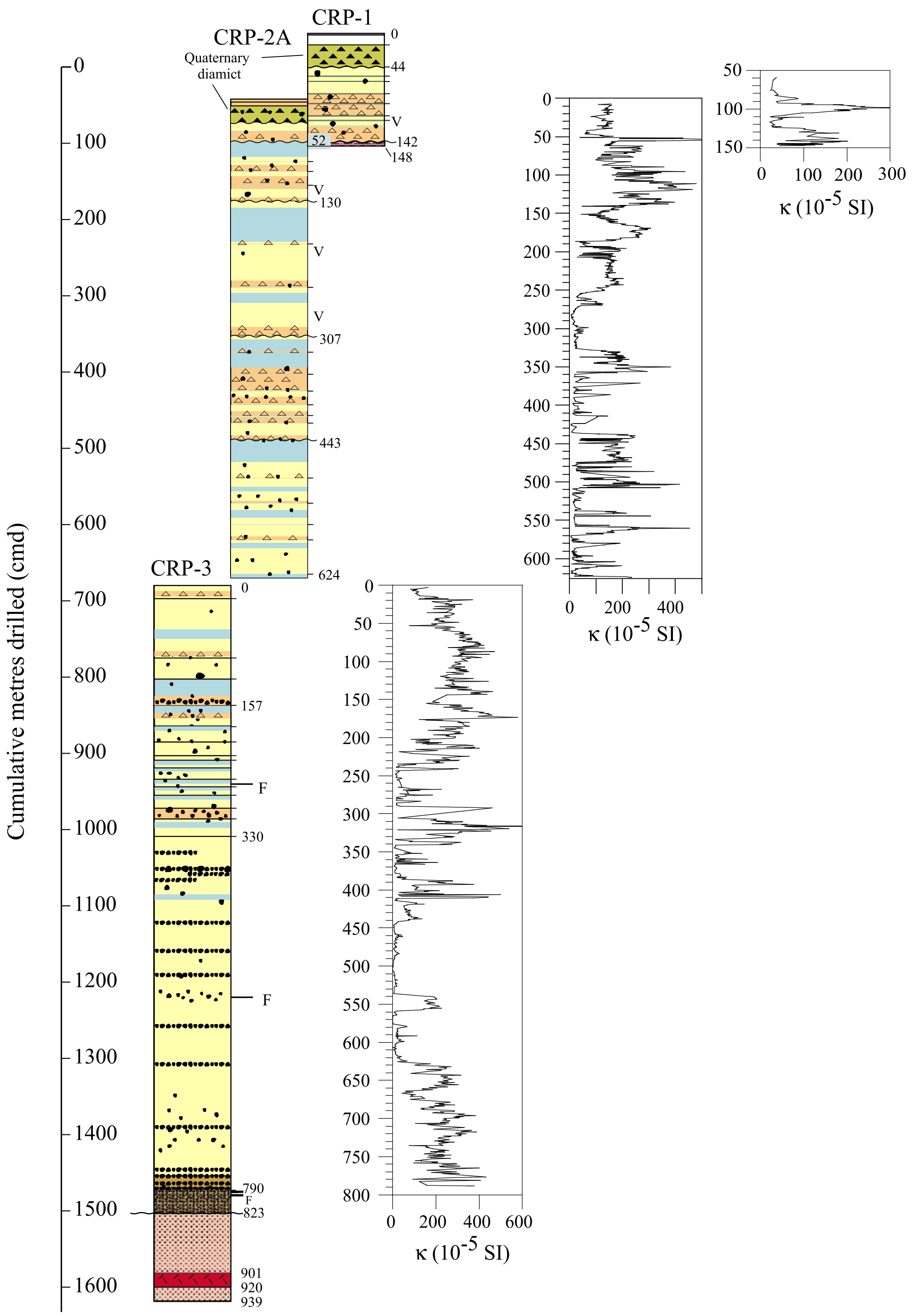

Fig. 4. Composite lithostratigraphic log for the CRP-1, CRP-2, and CRP-3 drill-cores (symbols as in Fig. 3) and down-core variations of magnetic susceptibility (κ).

part of the CRP-1 core to have resulted from a late diagenetic change in pore water conditions where abundant surficial iron in the siderite grains reacted with fluids containing limited dissolved sulphide, thereby causing precipitation of greigite (Sagnotti et al., 2005). This lowermost interval of the CRP-1 drill-core is the only part of the recovered CRP succession in which we have documented the presence of greigite and an associated remagnetization. It was not observed in the interval of equivalent age in the CRP-2 core.

3.2. CRP-2 drill-core

Magnetite, with some maghemite, is the dominant ferrimagnetic mineral in the upper 270 m of the CRP-2 drill-core (Verosub et al., 2000). Below 270 mbsf, the concentration-dependent parameters (i.e., κ, ARM, M_{rs}, and M_s) alternate between relatively high values and low background values (e.g., Fig. 4). Relatively higher coercivities are observed in intervals where the concentration of ferrimagnetic minerals is low, and lower coercivities are evident in intervals where ferrimagnetic mineral concentrations are high. Thermomagnetic analyses indicate that hematite is the high coercivity mineral and that (low titanium) magnetite is the dominant magnetic mineral in the zones with relatively lower coercivity (Verosub et al., 2000).

3.3. CRP-3 drill-core

Relatively low coercivities and thermomagnetic behaviour imply that magnetite and/or low-Ti titanomagnetite are the primary remanence carriers throughout the CRP-3 drill-core (Florindo et al., 2001; Sagnotti et al., 2001). There is no evidence for significant amounts of relatively high coercivity minerals (such as hematite) in the CRP-3 core, in contrast to our findings in the CRP-1 and CRP-2 cores (Sagnotti et al., 1998; Verosub et al., 2000). Hysteresis parameters are consistent with the presence of PSD magnetite in a narrow grain size range (cf. Day et al., 1977). No evidence of "wasp-waisted" characteristics was detected, which is consistent with a uniform magnetic mineralogy and a narrow range of grain sizes (cf. Roberts et al., 1995).

4. Results—palaeomagnetic behaviour

Demagnetization results were examined using orthogonal vector component diagrams, stereographic projections and intensity decay curves. ChRM components were determined from principal component analysis (Kirschvink, 1980), using data from multiple demagnetization steps. Most of the samples analysed from the CRP cores display a nearly vertical, normal polarity component that is interpreted to represent a drilling-induced overprint (Fig. 5a–c). This overprint has been observed in all of the cores that we have studied from the VLB (Roberts et al., 1998, 2003; Wilson et al., 1998, 2000a; Florindo et al., 2001). The presence of this overprint provided a further control to ensure that samples had not been inadvertently flipped during sampling and/or measurement. In some cases, the overprint and the original remanence had completely overlapping coercivity spectra, and it was not possible to discriminate between the two components (Fig. 5c). Such samples were excluded from magnetostratigraphic interpretations. Glacimarine sediments recovered in the CRP drill-cores often contain coarse sands and larger clasts (often dolerite clasts) within the matrix, and, when present in samples, they can give rise to spurious palaeomagnetic results (i.e., with abnormally low inclinations or multiple components of magnetization; e.g., Fig. 5b). Samples that exhibited this behaviour were also not included in the magnetostratigraphic interpretations.

The normal and reversed polarity ChRM inclinations from the remaining samples from the CRP-1, CRP-2, and CRP-3 drill-cores are grouped in two nearly antipodal clusters, as expected for reliable ChRM directions (Fig. 6). In conjunction with evidence from vector component diagrams (and a positive conglomerate test on an intraformational breccia from the CRP-2 drill-core), this indicates that secondary overprints have been successfully removed by stepwise AF demagnetization (Roberts et al., 1998; Wilson et al., 2000a; Florindo et al., 2001).

4.1. CRP-1 drill-core

The drilling-induced overprint is particularly strong in the low κ zones, which makes it difficult

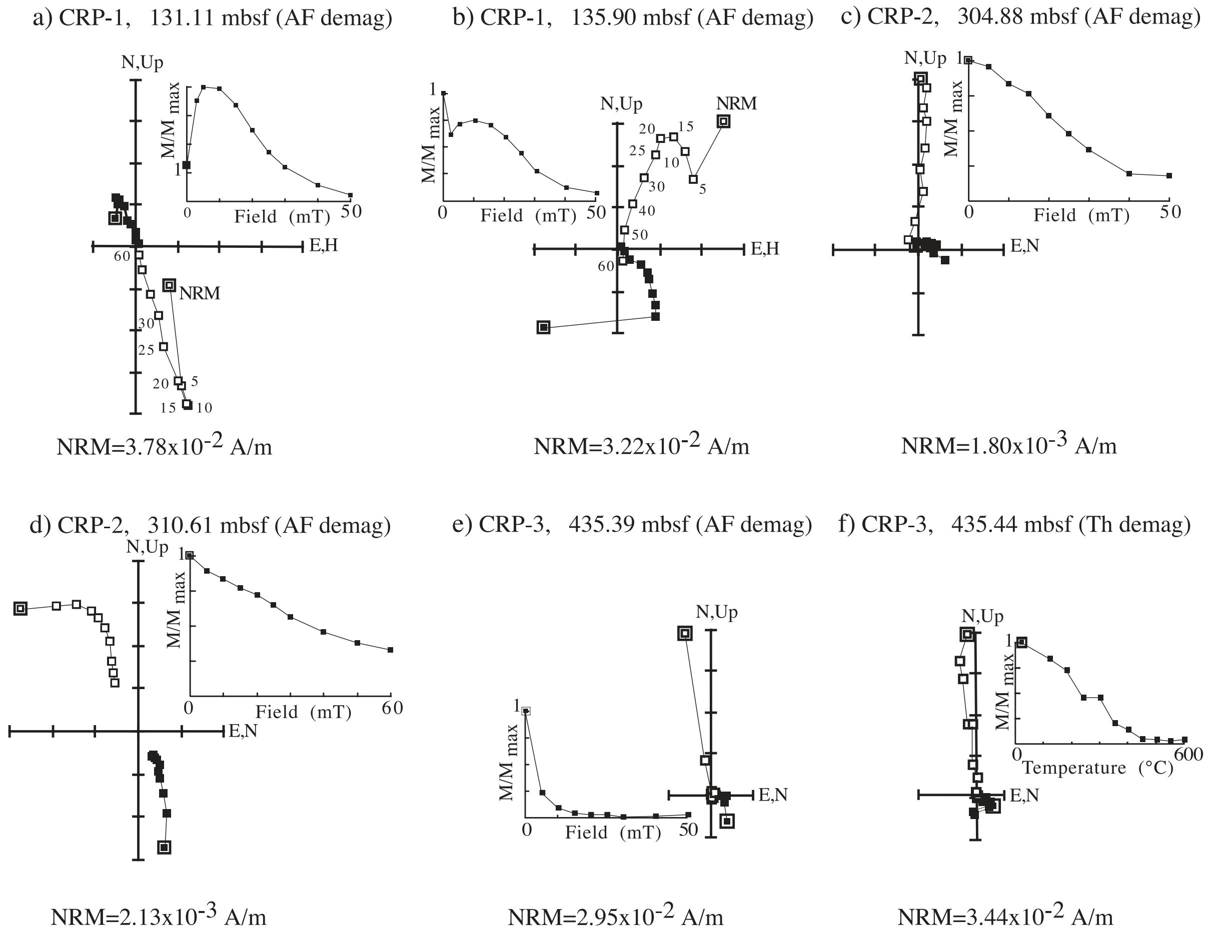

Fig. 5. Demagnetization behaviour for six representative samples from the CRP-1, CRP-2, and CRP-3 drill-cores. For the vector component diagrams, open (closed) symbols represent projections onto the vertical (horizontal) plane. Samples are not azimuthally oriented and declinations are reported in the laboratory coordinate system with respect to the split face of the drill-core. M=NRM intensity. See text for discussion.

to isolate a stable ChRM component with AF demagnetization. Thermal treatment was therefore used for many of the samples from these zones. Conversely, in the high κ zones, AF demagnetization at 5 or 10 mT was sufficient to remove this overprint (e.g., Fig. 5a). For most of the paired samples from the high κ intervals, thermal and AF demagnetization were equally effective in removing secondary magnetization components and in isolating identical ChRM components for both normal and reversed polarity. All other samples from the high κ intervals were treated with AF demagnetization. Stable palaeomagnetic behaviour is evident from the vector component plots of 140 of the 166 samples (Roberts et al., 1998).

4.2. CRP-2 drill-core

In some cases, particularly in sandy lithologies (e.g., 199.64–212.10 mbsf), another overprint is present in addition to the drilling induced overprint. This overprint has a consistently near-horizontal inclination and a declination that is directed away from the cut face of the drill-core (e.g., Fig. 5d). Magnetic field measurements at the CRP drill-site core preparation facility indicated that the overprint probably resulted from a relatively strong magnetic field produced by rotation of the saw blade that was used to split the drill-cores (Wilson et al., 2000a). When present, it replaces the viscous or drilling-induced overprint. In most cases, it can be removed by

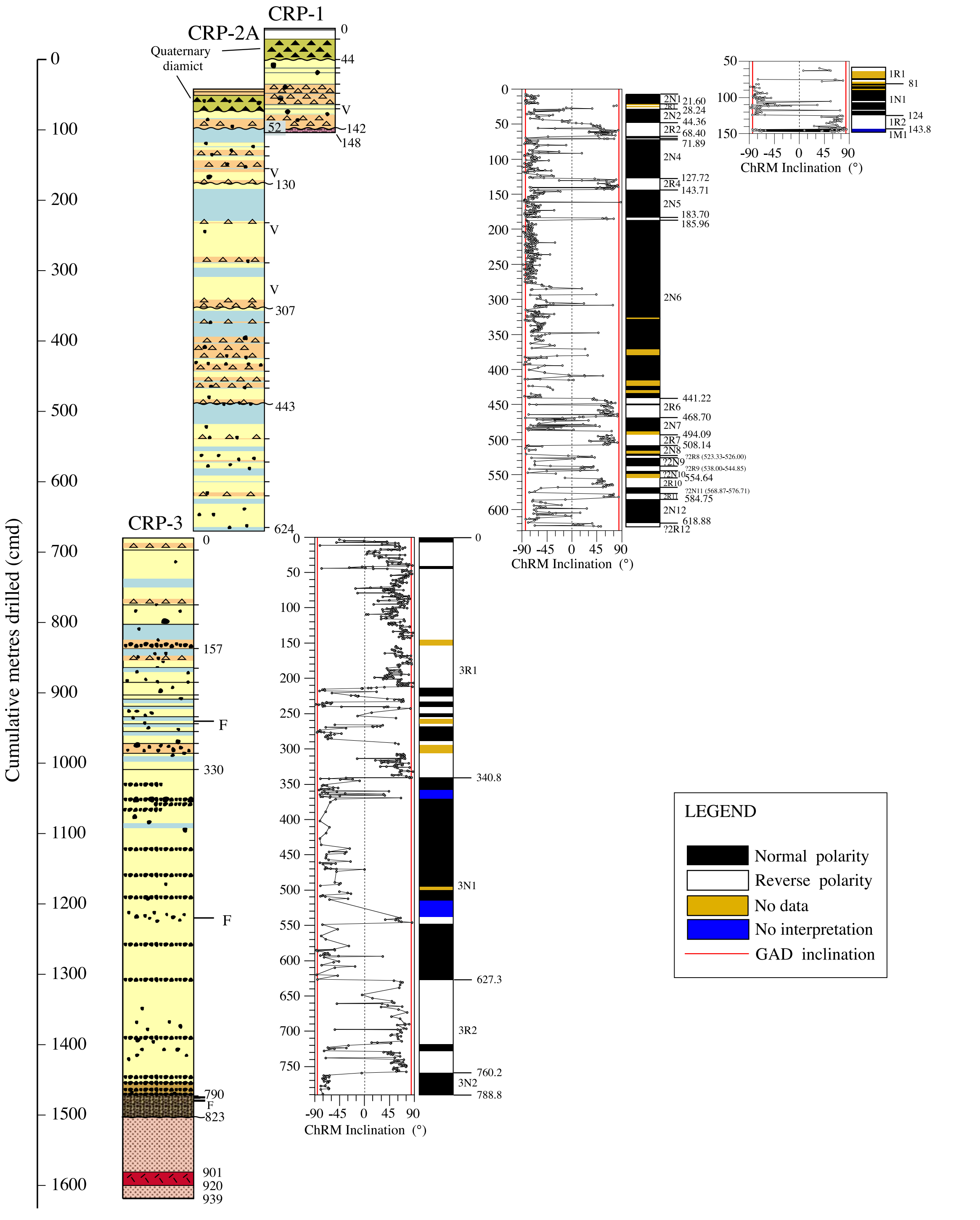

Fig. 6. Composite lithostratigraphic log for the CRP-1, CRP-2, and CRP-3 drill-cores (symbols as in Fig. 3), down-core variations of inclination of the characteristic remanent magnetization (ChRM), and magnetic polarity zonation (black=normal polarity, white=reverse polarity).

peak AFs of 10–20 mT. Stable palaeomagnetic behaviour was observed in 820 of the 963 samples analysed (Wilson et al., 2000a).

4.3. CRP-3 drill-core

Most of the samples analysed have a low-coercivity, nearly vertical, normal polarity component that was generally removed without difficulty with peak AFs of ≤20 mT. In a thick interval dominated by well-sorted and clean sandstones, from 380 to 580 mbsf, reliable polarity data were more difficult to obtain. In this interval, the pilot AF demagnetization study revealed a dominance of low-coercivity phases, consistent with the presence of coarse-grained magnetic minerals (Fig. 5e). Thermal demagnetization usually revealed a steep normal polarity component, which was gradually removed by heating to 400–500 °C (Fig. 5f). We interpreted this component as a viscous remanent magnetization that is relatively resistant to thermal demagnetization. Stable palaeomagnetic behaviour was identified in 635 of the samples from the Eocene–Oligocene succession in the CRP-3 drill-core (Florindo et al., 2001).

5. Results—magnetic polarity zonation

The magnetic polarity record of the CRP succession was subdivided into magnetozones, where magnetozones are defined as intervals with multiple, consecutive samples with inclinations that are distinctly different from neighbouring intervals (Fig. 6). In most cases, the magnetozones are defined by samples with inclinations that are antipodal compared to neighbouring magnetozones and with a clearly defined normal or reversed polarity. In many of the magnetozones, occasional isolated samples have polarities opposite to those of the rest of the magnetozone. In each case, the palaeomagnetic behaviour is stable and the presence of a steep normal polarity viscous or drilling-induced overprint suggests that the samples have not been inadvertently inverted. These samples are believed to represent short-period geomagnetic fluctuations, such as geomagnetic excursions, that are recorded in the CRP succession because of the high sediment accumulation rates (see below) combined with the high sampling density. Such isolated samples are not used to define polarity zones. Boundaries between magnetozones are placed either at the mid-point between successive samples of opposite polarity or at a lithological contact or disconformity that separates such samples. Magnetozones are labelled according to the CRP drill-core number (i.e., 1, 2, or 3), the polarity of the magnetozone (i.e., N or R), with progressive down-core numbering within the respective drill-hole (i.e., 1, 2, 3, etc.).

Some of the CRP magnetozones encompass several lithostratigraphic units and span possible stratigraphic disconformities, including sequence-bounding unconformities. These intervals have been treated with caution when interpreting the magnetic polarity stratigraphy because some of them appear to represent a juxtaposition of more than one polarity subchron (Roberts et al., 1998; Wilson et al., 1998, 2000a; Florindo et al., 2001).

5.1. CRP-1 magnetic polarity zonation

The polarity record was divided into four main magnetozones by Roberts et al. (1998; Fig. 6): an upper magnetozone with predominantly reversed polarity (<81 mbsf, 1R1); a predominantly normal polarity magnetozone from 81 to 124 mbsf (1N1), with two thin reversed polarity intervals at c. 106 and 118 mbsf, respectively; a third magnetozone with reversed polarity between 124 and 143.8 mbsf (1R2); and a magnetozone with mixed polarity at the base of the core, between 143.8 and 147.65 mbsf (1M1). All of the thin normal polarity intervals that comprise the mixed polarity magnetozone contain authigenic greigite, and are interpreted to carry a palaeomagnetic signal associated with a late diagenetic remagnetization event (Sagnotti et al., 2005). This mixed polarity interval is therefore not considered in our overall magnetostratigraphic interpretation.

5.2. CRP-2 magnetic polarity zonation

The succession recovered in the CRP-2 drill-core was subdivided into 24 magnetozones by Wilson et al. (2000a; Fig. 6): 12 with dominantly normal polarity and 12 with dominantly reversed polarity. Among these, three magnetozones, indicated by ?2R8, ?2R9, and ?2R12, have shallower inclinations than expected for reversed polarity samples at the latitude of the

CRP-2 drill-site (assuming a geocentric axial dipole field), and three magnetozones, indicated by ?2N9, ?2N10, and ?2N11, are defined by relatively few samples that are more widely spaced than samples from other magnetozones. All of these magnetozones have been treated with caution when interpreting the magnetic polarity stratigraphy.

The upper 435 m of the CRP-2 drill-core is dominated by normal polarity. The most likely explanation for this is a high sediment accumulation rate, and/or that more than one normal polarity chron is juxtaposed at one or more of the many stratigraphic disconformities in this glacimarine succession (Cape Roberts Science Team, 1999). A significant number of discrete samples have inclinations that are intermediate between normal and reversed polarity. In the majority of cases, these samples appear to be consistent with the presence of geomagnetic polarity transitions. The best example of this can be found between 43 and 50 mbsf, where a transition from reversed to normal polarity is recorded across a lithostratigraphic boundary between a diamicton unit and a sand unit. Recording of significant thicknesses of intermediate polarity directions suggests that sediment accumulation rates were high.

A thick interval of normal polarity between 185.96 and 441.22 mbsf is designated as a single normal polarity magnetozone (2N6). This magnetozone separates the magnetic polarity record of CRP-2 into 3 sub-equal intervals: a 186-m-thick upper interval of alternating normal and reversed polarity (magnetozones 2N1–2R5); a middle 255-m-thick interval comprising a single normal polarity magnetozone (2N6); and a lower 183-m-thick interval of alternating normal and reversed polarity (magnetozones 2R6–?2R12).

5.3. CRP-3 magnetic polarity zonation

The succession recovered in the CRP-3 drill-hole was subdivided into four main magnetozones by Florindo et al. (2001; Fig. 6): two with dominantly reversed polarity (3R1 and 3R2) and two with dominantly normal polarity (3N1 and 3N2). The upper 340.8 m of the magnetic polarity record is dominated by reversed polarity (magnetozone 3R1), although it contains some thin intervals with shallow reversed or normal polarity inclinations. Magnetozone 3N1 is a thick zone of normal polarity between 340.8 and 627.3 mbsf. In the upper part of magnetozone 3N1, from 359.3 to 370.4 mbsf, a mixed polarity zone is evident in which most of the inclination fluctuations are represented by single samples. Polarity is not interpreted for this interval. From 513.49 to 539.63 mbsf, the magnetizations are weak and the sediments are coarse-grained; no reliable ChRM inclinations were obtained for this 26-m-thick interval. A normal fault occurs at 539.31 mbsf, which marks the upper boundary of an 8-m-thick interval of reversed polarity within magnetozone 3N1. Reversed polarity dominates the interval from 627.3 to 760.2 mbsf (magnetozone 3R2). From 718.64 to 728.68 mbsf, there is a normal polarity interval that is defined by six samples. Shallow inclinations are recorded by two samples at 648.21 and 653.12 mbsf, which may represent part of another thin normal polarity interval; however, other samples near this level did not yield stable magnetizations. The lower 31 m of the CRP-3 late Eocene–Oligocene succession comprises stable normal polarity (magnetozone 3N2). The lower boundary of magnetozone 3N2 was not reached above the dolerite conglomerate at 790 mbsf. The lowermost sample with stable palaeomagnetic behaviour in the Eocene–Oligocene succession was collected at 788.82 mbsf.

6. Magnetostratigraphic chronology for the CRP succession

6.1. The composite Eocene–Miocene CRP succession

The Eocene–Miocene succession recovered by CRP drilling has a thickness of 1472 m in cumulative metres drilled (cmd). This thickness was calculated by combining the non-overlapping sediment thicknesses from each of the three CRP cores (Table 1). Seismic reflection (Fig. 2) and age data indicate that there is an overlap of ca. 31 m between the base of the Miocene succession in CRP-1 and the upper part of the Miocene succession recovered in CRP-2 and that there is a gap of some tens of metres between the base of the CRP-2 core and the top of the CRP-3 core (Cape Roberts Science Team, 2000). The overlap of 31 m between the CRP-1 and CRP-2 cores is calculated by correlation of a common unconformity surface recovered in the two cores. However, the large number of unconformities in the CRP succession and the offsets between the

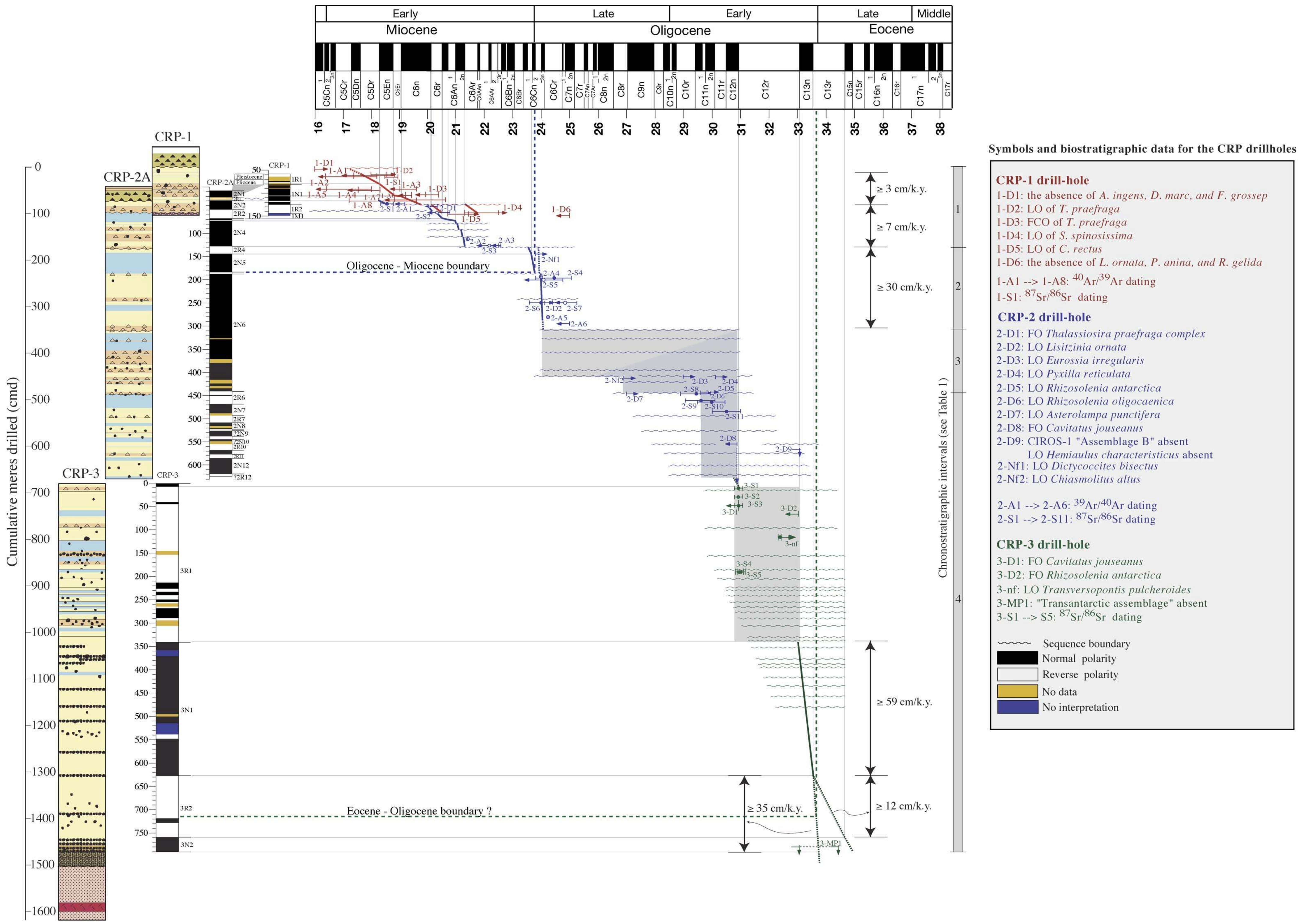

Fig. 7. Composite lithostratigraphic log for the CRP-1, CRP-2, and CRP-3 drill-cores (symbols as in Fig. 3) and correlation of the composite magnetic polarity zonation with the GPTS of Cande and Kent (1995) and Berggren et al. (1995). Black (white) denotes normal (reversed) polarity. Undulating lines represent sequence-bounding unconformities where time loss is predicted based on lithostratigraphic evidence. Solid lines indicate our preferred age–depth correlation. The light grey shading indicates the range of possible age–depth correlations based on biostratigraphic and other data.

Table 1
Cumulative depths for the CRP Eocene–Miocene succession

Age		CRP-1 mbsf	CRP-1 cmd	CRP-2 mbsf	CRP-2 cmd	CRP-3 mbsf	CRP-3 cmd	Eo - Miocene age model subdivisions
Cenozoic	Quaternary	0.00 43.55		5.54 26.79				
Cenozoic	Early Miocene	43.55 | 141.60	0.00 | 98.05	26.79 | 52.63	98.05			1
Cenozoic	Early Miocene	147.69		52.63 | 130.27	98.05 | 175.69			1
Cenozoic	Early Miocene			130.27 | 183.70	175.69 | 229.12			2
Cenozoic	Oligocene			183.70 306.65	229.12 352.07			2
Cenozoic	Oligocene			306.65 442.99	352.07 488.41			3
Cenozoic	Oligocene			442.99 624.15	488.41 669.57			4
Cenozoic	Oligocene					2.80 |	669.57 |	4
Cenozoic	Eocene?					805.60	1472.37	4
Mesozoic						805.60 939.42		
mbsf to cmd conversion:		subtract 43.55 m		add 45.42 m		add 666.77 m		

The shaded intervals indicate the core intervals included in the composite CRP Eocene–Miocene succession.

successive drill-holes result in different lithofacies and sedimentation rates for the respective cores, so that it is not possible to correlate directly between the overlapping intervals in the cores. We have therefore chosen to construct the composite depth succession for the three CRP cores simply by joining the successions recovered in the CRP-1 and CRP-2 cores at the correlated unconformity and by joining the top of the CRP-3 succession to the base of the CRP-2 succession (Table 1). In doing this, we recognise that our composite succession will be fragmented by numerous unconformities.

6.2. Age model for the composite Eocene–Miocene CRP succession

In the following discussion, we provide an interpretation of the magnetic polarity pattern for the Eocene–Miocene CRP succession. Correlation to the geomagnetic polarity time scale (GPTS) is constrained by a number of $^{40}Ar/^{39}Ar$ and $^{87}Sr/^{86}Sr$ ages obtained from both in situ and reworked materials (Lavelle, 1998, 2000, 2001; McIntosh, 1998, 2000; Wilson et al., 2002), by a new Antarctic siliceous microfossil zonation (Harwood et al., 1998; Scherer et al., 2000; Harwood and Bohaty, 2001) and by calcareous nannoplankton biostratigraphy (Watkins and Villa, 2000; Watkins et al., 2001). Other microfossil groups play a limited role in constraining the age of the Eocene–Miocene interval of the CRP succession. For discussion, it is useful to divide the succession into four chronostratigraphic intervals (Table 1 and Fig. 7).

6.2.1. Subdivision 1 (0.00–175.69 cmd): early Miocene

The upper part of the CRP succession is characterized by thin (10–20 m in thickness) sedimentary sequences and by thicker magnetozones that usually span sequence-bounding unconformities. The lower Miocene interval is dominated by two normal polarity magnetozones (1N1 and 2N4) that are separated by a ~30-m-thick reversed polarity magnetozone that spans the unconformity observed in both the CRP-1 and CRP-2 drill-cores (magnetozones 1R2 and 2R2). Correlation to the GPTS is constrained by a number of $^{40}Ar/^{39}Ar$ and $^{87}Sr/^{86}Sr$ dates as well as by several diatom datums (Fig. 7).

Roberts et al. (1998) could not make a unique correlation to the GPTS for magnetozone 1N1, but with drilling of CRP-2, a new $^{87}Sr/^{86}Sr$ date (18.62±0.22 Ma) from a solitary coral (Lavelle, 2000) at 81.67 cmd (S1) in CRP-2 suggests a unique correlation for magnetozone 1N1 with Chron C5En and that the short intervals of reversed polarity within the dominantly normal magnetozone must represent geomagnetic excursions. An $^{40}Ar/^{39}Ar$ age (21.44±0.05 Ma) for an ash horizon at 158 cmd (A2) constrains correlation of the base of magnetozone 2N4 to Chron C6An.2n (Wilson et al., 2000a). The numerous unconformities within the upper part of magnetozone 2N4 prevent unique correlation with the GPTS. This part of magnetozone 2N4 could correlate with chrons C6An.1n and/or C6An.2n (Fig. 7). However, the overlying unconformity at 98.05 cmd, which is interpreted to occur in both the CRP-1 and CRP-2 drill-holes, could also represent a ~2 m.y. hiatus between chrons C5En and C6An.2n.

6.2.2. Subdivision 2 (175.69–352.07 cmd): Oligocene–Miocene boundary

The Oligocene–Miocene boundary interval is an extremely well-dated interval in the VLB; thick successions of this age have been recovered in the CRP-2 core (Wilson et al., 2000a,b, 2002; Naish et al., 2001) and in the nearby CIROS-1 core (Roberts et al., 2003). In the CRP-2 core, this interval comprises three ~60-m-thick sedimentary sequences and a N–R–N–R magnetic polarity sequence that includes the upper part of magnetozone 2N6, magnetozones 2R5 and 2N5, and the lower part of magnetozone 2R4, which are correlated with chrons C6Cn.3n–C6Cn.1r, respectively (Wilson et al., 2000a; Fig. 7). The Oligocene–Miocene boundary occurs at the C6Cn.2r–C6Cn.2n polarity transition, which lies at 229.12 cmd in the CRP succession. Four $^{87}Sr/^{86}Sr$ dates, two from in situ articulated bivalves and two from reworked bivalve fragments, and two biostratigraphic datums constrain the correlation. The resulting magnetostratigraphy is in turn calibrated by $^{40}Ar/^{39}Ar$ dates on two tephra layers at 239 and 325 cmd (23.98±0.13 and 24.22±0.03 Ma), respectively. Wilson et al. (2002) concluded that the chronostratigraphy for this interval was of sufficient resolution and precision to afford a new calibration for the Oligocene–Miocene boundary.

6.2.3. Subdivision 3 (352.07–488.41 cmd): late Oligocene?

Numerous unconformities, lack of independent age control, and the complexity of the GPTS in the Late Oligocene prevented Wilson et al. (2000a) from correlating the solely normal polarity of this interval (part of Magnetozone 2N6) with the GPTS. Correlation cannot be specifically constrained to any of the normal polarity subchrons over a 6-m.y. interval from chrons C11n.2n to C6Cn.3n. At best, therefore, it is only possible to say that this interval appears to be of Late Oligocene age and that one or more of the unconformities in this interval were probably of significant duration.

6.2.4. Subdivision 4 (488.41–1472.37 cmd): latest Eocene?–early Oligocene

Poor age control, along with a complex magnetic polarity stratigraphy, in the lower part of the CRP-2 drill-hole prevented Wilson et al. (2000a,b) from developing a unique age model for the interval between 488.41 and 669.57 cmd. Some refinement, however, is possible following drilling of the CRP-3 drill-hole. The dominance of reversed polarity, along with diatom and nannofossil biostratigraphic constraints and five $^{87}Sr/^{86}Sr$ dates, one from an in situ articulated bivalve and the others from reworked bivalve fragments, suggests that the interval between 669.57 and 1007.57 cmd (magnetozone 3R1) correlates with part of Chron C12r (Florindo et al., 2001). Thus, the overlying interval (488.41–669.57 cmd) of complex polarity must correlate with Chron C12n and/or younger subchrons. $^{87}Sr/^{86}Sr$ dates from in situ articulated bivalves at 490.46 (29.4±0.5 Ma) and 508.79 cmd (29.9±0.5 Ma) suggest that the lower part of magnetozone 2R6 and magnetozones 2N7 to 2N12 correlate with chrons C10n.1r–C12n (Fig 7; option B of Wilson et al., 2000a,b). The correlation is, however, not a perfect match and assumes that some of the thinner magnetozones represent geomagnetic excursions or short polarity intervals that might correspond to "tiny wiggles" (Cande and Kent, 1992a,b) on marine magnetic anomaly records (e.g., Roberts and Lewin-Harris, 2000).

Below 1007.57 cmd, two main magnetozones are recognized (3N1 and 3R2; Fig. 7). Each of these magnetozones also contains thin opposite polarity intervals that Florindo et al. (2001) interpreted to represent geomagnetic excursions or short polarity intervals corresponding to cryptochrons in the GPTS (Cande and Kent, 1992a,b, 1995). Correlation to the GPTS is hampered by the paucity of independent age data between 1007.57 and 1472.37 cmd. The one exception is an interval of high marine palaeoproductivity between 1448.01 and 1455.46 cmd, which yielded a diverse marine palynomorph flora (Hannah et al., 2001a,b). While the recovered assemblage is not directly age diagnostic, it does not contain species identified to represent the mid-late Eocene Transantarctic Flora (Wrenn and Hart, 1988). Hence, magnetozones 3N1 and 3R2 are correlated with chrons C13n and C13r, respectively. It is not possible at this stage to know whether magnetozone 3N2 correlates with Chron C15n or whether it represents a cryptochron.

7. Discussion

7.1. Sediment accumulation rates and Victoria Land Basin subsidence history

The age of the strata in the CRP-3 drill-core, just above the unconformity that separates these strata from the Devonian Beacon Supergroup, probably represents the age of a major rifting event that formed this section of the VLB and that was contemporaneous with, and probably related to, sea floor spreading in the Adare Trough, north of the northern Victoria Land continental margin (Cande et al., 2000). This evidence, associated with the great thickness of Oligocene strata recovered in the CRP-2 and CRP-3 drill-holes, indicates that rapid basin subsidence began, with concomitant abundant sediment supply, no later than during latest Eocene–earliest Oligocene times. In particular, the slope of the correlation line on Fig. 7 indicates a period of rapid sediment accumulation from ~34–35 to ~28 Ma (late Eocene–early Oligocene). The sediment accumulation rate decreased significantly during the early Miocene, from ~21 to ~17.5 Ma. This evidence is consistent with studies of basin subsidence (De Santis et al., 2000, 2001), which suggest an Oligocene age of rift basin formation in the vicinity of Cape Roberts.

7.2. Antarctic glacial history as recorded at the CRP sites

A cumulative thickness of 1472 m of strata was recovered in the three CRP drill-holes. These strata provide a discontinuous record of late Eocene to early Miocene (~35 to ~17 Ma) sedimentation and palaeoclimate variation. We have subdivided the Eocene–Miocene succession into four unconformity-bounded chronostratigraphically defined intervals (1. 0.00–175.69 cmd; 2. 175.69–352.07 cmd; 3. 352.07–488.41; and 4. 488.41–1472.37 cmd). These intervals are characterized by different average sediment accumulation rates and by unconformity-bounded sedimentary cycles that indicate progressive changes in the environment of deposition and associated climate.

While much of the CRP-3 core (669.57–1472.37 cmd) is represented by early syn-rift sedimentation with poor chronostratigraphic control, it is important to note that the preglacial, middle Eocene strata, identified by the Transantarctic dinoflagellate assemblage of Wrenn and Hart (1988), were not recovered in the CRP succession. Neither was a distinctive event encountered that might represent a build-up of Antarctic glaciation at the Eocene–Oligocene boundary, as indicated by oxygen isotope records from deep-sea sediments (e.g., Zachos et al., 2001).

The time interval between ~33 and 24.3 Ma (from the upper part of C13n to the upper part of Chron C6Cr) is represented by a major unconformity in the CIROS-1 drill-core (see chronology of Roberts et al., 2003) that has been interpreted to represent a significant expansion of the EAIS which extended well offshore into the Ross Sea (Harwood et al., 1989; Bartek et al., 1996; Wilson et al., 1998; Roberts et al., 2003). The same time interval is represented by a substantial thickness of sediment in the CRP-2 and CRP-3 drill-holes. It is likely that a major unconformity observed at 352.07 cmd in CRP-2 (306.65 mbsf), where a marked change in sediment provenance also occurs, is responsible for the absence of much of the Late Oligocene record. However, the Early Oligocene is still represented by at least 800 m of strata in the CRP succession. This difference in sediment thickness across the VLB probably reflects differences in the palaeo-topographic position of the respective drill sites with respect to sea level and to glacial erosion. Nevertheless, the major unconformity at 352.07 cmd in the CRP succession could be a stratigraphic expression of the same erosive event as documented in the CIROS-1 drill-core, although poor age control below 352.07 cmd prevents us from estimating the time interval represented by the unconformity in the CRP succession.

The Oligocene–Miocene boundary interval (spanning the Mi-1 $\delta^{18}O$ glacial event) is well represented in the CRP succession (Interval 2; 175.69–352.07 cmd) and includes thick unconformity-bound glacimarine cycles that persist throughout the remainder of the CRP Miocene succession (Cape Roberts Science Team, 1999; Naish et al., 2001). The precision of our dating of this multiphase glacial episode makes the Mi-1 event the first Neogene or Palaeogene deep-sea $\delta^{18}O$ glacial event to be recognized and precisely identified in Antarctic margin sediments.

The unconformity that separates intervals 1 and 2 at 175.69 cmd had a duration of more than 2 m.y. (encompassing chrons C6Br-C6Ar). The top of the unconformity might correlate with the Mi-1a $\delta^{18}O$ event; however, the isotopic excursion reported by Miller et al. (1991) is not as positive as the Mi-1 event nor has a coeval sequence boundary been identified for the Mi-1a event on the New Jersey margin (Miller et al., 1991).

Acknowledgements

The Cape Roberts Project was made possible through the resources and close collaboration of the Antarctic programmes of Australia, Germany, Italy, New Zealand, The Netherlands, United Kingdom, and the United States of America. We thank all of our colleagues from the Cape Roberts Science Team and the people of McMurdo Station, Scott Base and Cape Roberts Camp for logistical support. The palaeomagnetic component of the Cape Roberts Project was supported by grants from the Italian Programma Nazionale di Ricerche in Antartide to FF and LS, from the U.S. National Science Foundation to KLV, APR, and GSW, and from the New Zealand Foundation for Research to GSW. We are grateful to Adam Harris, Alfredo Sorice, and Betty Trummel for their help in the laboratory at McMurdo Station. We appreciate the insightful reviews and comments by Peter Barrett and Stefanie Brachfeld on an earlier version of the manuscript.

References

Armstrong, R.L., 1978. K–Ar dating: late Cenozoic McMurdo volcanic group and Dry Valley glacial history, Victoria Land, Antarctica. New Zealand Journal of Geology and Geophysics 21, 685–698.

Baker, J.C., Fielding, C.R., 1998. Diagenesis of glacimarine Miocene strata in CRP-1, Antarctica. Terra Antartica 5, 647–653.

Barrett, P.J., 1981. History of the Ross Sea region during the deposition of the Beacon Supergroup 400–180 million years ago. Journal of the Royal Society of New Zealand 11, 447–458.

Barrett, P.J., Davey, F.J. (Eds.), 1992. Antarctic Stratigraphic Drilling: Cape Roberts Project Workshop Report, The Royal Society of New Zealand Miscellaneous Series, vol. 23. The Royal Society of New Zealand, Wellington, 38 pp.

Barrett, P.J., et al., (Eds.), 2000. Studies from the Cape Roberts Project, Ross Sea, Antarctica. Scientific Results of CRP-2/2A, Parts I and II. Terra Antartica, vol. 7, pp. 1–665.

Barrett, P.J., et al., (Eds.), 2001. Studies from the Cape Roberts Project, Ross Sea, Antarctica. Scientific Results of CRP-3, Parts I and II. Terra Antartica, vol. 8, pp. 1–621.

Bartek, L.R., Henrys, S.A., Anderson, J.B., Barrett, P.J., 1996. Seismic stratigraphy of McMurdo Sound, Antarctica: implications for glacially influenced early Cenozoic eustatic change? Marine Geology 130, 79–98.

Berggren, W.A., Kent, D.V., Swisher III, C.C., Aubrey, M.P., 1995. A revised Cenozoic geochronology and biostratigraphy. In: Berggren, W.A., Kent, D.V., Aubrey, M.P., Hardenbol, J. (Eds.), Geochronology, Time Scales, and Stratigraphic Correlation. Society of Economic Paleontologists and Mineralogists, Special Publication, vol. 54, pp. 129–212.

Brancolini, G., Busetti, M., Marchetti, A., DeSantis, L., Zanolla, C., Cooper, A.K., Cochrane, G.R., Zayatz, I., Belyaev, V., Knyazev, M., Vinnikovskaya, O., Davey, F.J., Hinz, K., 1995. Descriptive text for the seismic stratigraphy atlas of the Ross Sea. In: Cooper, A.K., Barker, P.F., Brancolini, G. (Eds.), Geology and Seismic Stratigraphy of the Antarctic Margin. Antarctic Research Series, vol. 68. AGU, Washington, DC, pp. A268–A271.

Cande, S.C., Kent, D.V., 1992a. A new geomagnetic polarity time scale for the Late Cretaceous and Cenozoic. Journal of Geophysical Research 97, 13917–13951.

Cande, S.C., Kent, D.V., 1992b. Ultrahigh resolution marine magnetic anomaly profiles: a record of continuous paleointensity variations? Journal of Geophysical Research 97, 15075–15083.

Cande, S.C., Kent, D.V., 1995. Revised calibration of the geomagnetic polarity time scale for the Late Cretaceous and Cenozoic. Journal of Geophysical Research 100, 6093–6095.

Cande, S.C., Stock, J.M., Muller, R.D., Ishihara, T., 2000. Cenozoic motion between East and West Antarctica. Nature 404, 145–150.

Cape Roberts Science Team, 1998. Initial Report on CRP-1, Cape Roberts Project, Antarctica. Terra Antartica 5, 187 pp.

Cape Roberts Science Team, 1999. Studies from the Cape Roberts Project, Ross Sea, Antarctica. Initial Report on CRP-2/2A. Terra Antartica 6 1–173. With Supplement, 245 pp.

Cape Roberts Science Team, 2000. Studies from the Cape Roberts Project, Ross Sea, Antarctica. Initial Report on CRP-3. Terra Antartica 7, 1–209. With Supplement, 305 pp.

Claps, M., Aghib, F.S., 1998. Carbonate diagenesis in Miocene sediments from CRP-1, Victoria Land basin, Antarctica. Terra Antartica 5, 655–660.

Cooper, A.K., Davey, F.J., Behrendt, J.C., 1987. Seismic stratigraphy and structure of the Victoria Land Basin, Western Ross Sea, Antarctica. In: Cooper, A.K., Davey, F.J. (Eds.), The Antarctic Continental Margin: Geology and Geophysics of the Western Ross Sea. Earth Science Series, vol. 5B. Circum-Pacific Research Council, Houston, TX, pp. 27–76.

Davey, F.J., Bennett, D.J., Houtz, R.E., 1982. Sedimentary basins of the Ross Sea, Antarctica. New Zealand Journal of Geology and Geophysics 25, 245–255.

Davey, F.J., Hinz, K., Schroeder, H., 1983. Sedimentary basins of the Ross Sea, Antarctica. In: Oliver, R.L., James, P.R., Jago, J.B. (Eds.), Antarctic Earth Science. Australian Academy of Science, Canberra, pp. 533–588.

Davey, F.J., Barrett, P.J., Cita, M.B., van der Meer, J.J.M., Tessensohn, F., Thomson, M., Webb, P.-N., Woolfe, K.J., 2001. Drilling for Antarctic Cenozoic climate and tectonic history at Cape Roberts, southwestern Ross Sea. EOS, Transactions-American Geophysical Union 82 (48), 585.

Day, R., Fuller, M., Schmidt, V.A., 1977. Hysteresis properties of titanomagnetites: grain-size and compositional dependence. Physics of the Earth and Planetary Interiors 13, 160–267.

De Santis, L., Prato, S., Brancolini, G., Lovo, M., Torelli, L., 2000. The eastern Ross Sea continental shelf during the Cenozoic: implications for the West Antarctic ice sheet development. In: Van der Wateren, F.M., Cloetingh, S.A.P.L. (Eds.), Lithosphere Dynamics and Environmental Change of the Cenozoic West Antarctic Rift System. Global and Planetary Change, 23, 173–196.

De Santis, L., Davey, F.J., Prato, S., Brancolini, G., 2001. Subsidence at the Cape Roberts Project (CRP) drillsite from backstripping techniques, Victoria Land Basin, Antarctica. Terra Antartica 8, 137–141.

Fitzgerald, P.G., 1992. The Transantarctic Mountains of southern Victoria Land: the application of apatite–fission track analysis to a rift shoulder uplift. Tectonics 11, 634–662.

Florindo, F., Sagnotti, L., Roberts, A.P., Verosub, K.L., Wilson, G.S., 1997. The world's southernmost paleomagnetic laboratory is established in McMurdo Station (166°40′10″E, 77°50′18″S), Antarctica. EOS, Transactions-American Geophysical Union 78, 603.

Florindo, F., Wilson, G.S., Roberts, A.P., Sagnotti, L., Verosub, K.L., 2001. Magnetostratigraphy of late Eocene–early Oligocene strata from the CRP-3 core, McMurdo Sound, Ross Sea, Antarctica. Terra Antartica 8, 599–613.

Gunn, B.M., Warren, G., 1962. Geology of Victoria Land between Mawson and Mullock glaciers, Antarctica. New Zealand Geological Survey Bulletin 71.

Hambrey, M.J., et al., (Eds.), 1998. Studies from the Cape Roberts Project, Ross Sea, Antarctica. Scientific Results of CRP-1. Terra Antartica 5, 255–713.

Hamilton, R.J., Luyendyk, B.P., Sorlien, C.C., Bartek, L.A., 2001. Cenozoic tectonics of the Cape Roberts rift basin and Transantarctic Mountain front, southwestern Ross Sea, Antarctica. Tectonics 20, 325–342.

Hannah, M.J., Florindo, F., Harwood, D.M., Fielding, C.R., Cape Roberts Science Team, 2001a. Chronostratigraphy of the CRP-3 drillhole, Victoria Land Basin, Antarctica. Terra Antartica 8, 615–620.

Hannah, M.J., Wrenn, J.H., Wilson, G.J., 2001b. Preliminary report on early Oligocene and latest Eocene marine palynomorphs from CRP-3 drillhole, Victoria Land Basin, Antarctica. Terra Antartica 8, 383–388.

Harrington, H.J., 1958. Nomenclature of rock units in the Ross Sea region, Antarctica. Nature 182, 290.

Harwood, D.M., Bohaty, S.M., 2001. Early Oligocene siliceous microfossil biostratigraphy of Cape Roberts Project core CRP-3, Victoria Land Basin, Antarctica. Terra Antartica 8, 315–338.

Harwood, D.M., Barrett, P.J., Edwards, A.R., Rieck, H.J., Webb, P.-N., 1989. Biostratigraphy and chronology. In: Barrett, P.J. (Ed.), Antarctic Cenozoic history from the CIROS-1 drillhole, McMurdo Sound, Antarctica. Department of Scientific and Industrial Research Bulletin vol. 245. DSIR Publishing, Wellington, NZ, pp. 231–239.

Harwood, D.M., Bohaty, S.M., Scherer, R.P., 1998. Lower Miocene diatom biostratigraphy of the CRP-1 drillcore, McMurdo Sound, Antarctica. Terra Antartica 5, 499–514.

Henrys, S.A., Bucker, C.J., Niessen, F., Bartek, L.R., 2001. Correlation of seismic reflectors with the CRP-3 drillhole, Victoria Land Basin, Antarctica. Terra Antartica 8, 127–136.

Houtz, R., Davey, F.J., 1973. Seismic profiler and sonobuoy measurements in Ross Sea, Antarctica. Journal of Geophysical Research 78, 3448–3468.

Kirschvink, J.L., 1980. The least-squares line and plane and the analysis of palaeomagnetic data. Geophysical Journal of the Royal Astronomical Society 62, 699–718.

Kyle, P.R., 1990. McMurdo Volcanic Group—Western Ross embayment: introduction. Antarctic Research Series 48, 19–25.

Lavelle, M., 1998. Strontium–isotope stratigraphy of the CRP-1 drill-hole, Ross Sea, Antarctica. Terra Antartica 5, 691–696.

Lavelle, M., 2000. Strontium-isotope stratigraphy and age model for CRP-2/2A, Victoria Land Basin, Antarctica. Terra Antartica 7, 611–620.

Lavelle, M., 2001. Strontium-isotope stratigraphy for CRP-3, Victoria Land Basin, Antarctica. Terra Antartica 8, 593–598.

Mayewski, P.A., 1975. Glacial Geology and the late Cenozoic history of the Transantarctic Mountains, Institute of Polar

Studies Report, 56, 168 pp. Institute of Polar Studies, The Ohio State University, Columbus, OH, USA.
McIntosh, W.C., 1998. ^{40}Ar/^{39}Ar geochronology of volcanic clasts and pumice in CRP-1 core, Cape Roberts, Antarctica. Terra Antartica 5, 683–690.
McIntosh, W.C., 2000. ^{40}Ar/^{39}Ar geochronology of tephra and volcanic clasts in CRP-2A core, Victoria Land Basin, Antarctica. Terra Antartica 7, 621–630.
McKelvey, B.C., Webb, P.-N., Harwood, D.M., Mabin, M.C.G., 1991. The Dominion Range Sirius Group: a record of the Late Pliocene–Early Pleistocene Beardmore Glacier. In: Thomson, M.R.A., Crame, J.A., Thomson, J.W. (Eds.), Geological Evolution of Antarctica. Cambridge University Press, Cambridge, UK, pp. 675–682.
Mercer, J.H., 1968. Glacial geology of the Reedy Glacier area, Antarctica. Geological Society of America Bulletin 79, 471–485.
Miller, K.G., Wright, J.D., Fairbanks, R.G., 1991. Unlocking the ice house: Oligocene–Miocene oxygen isotopes, eustasy, and margin erosion. Journal of Geophysical Research 96, 6829–6848.
Naish, T.R., Woolfe, K.J., Barrett, P.J., Wilson, G.S., Atkins, C., Bohaty, S.M., Bücker, C.J., Claps, M., Davey, F.J., Dunbar, G.B., Dunn, A.G., Fielding, C.R., Florindo, F., Hannah, M.J., Harwood, D.M., Henrys, S.A., Krissek, L., Lavelle, M., van der Meer, J., McIntosh, W.C., Niessen, F., Passchier, S., Powell, R.D., Roberts, A.P., Sagnotti, L., Scherer, R.P., Strong, C.P., Talarico, F., Verosub, K.L., Villa, G., Watkins, D.K., Webb, P.-N., Wonik, T., 2001. Orbitally induced oscillations in the East Antarctic Ice Sheet at the Oligocene/Miocene boundary. Nature 413, 719–723.
Roberts, A.P., 1995. Magnetic properties of sedimentary greigite (Fe_3S_4). Earth and Planetary Science Letters 134, 227–236.
Roberts, A.P., Lewin-Harris, J.C., 2000. Marine magnetic anomalies: evidence that "tiny wiggles" represent short-period geomagnetic polarity intervals. Earth and Planetary Science Letters 183, 375–388.
Roberts, A.P., Cui, Y.L., Verosub, K.L., 1995. Wasp-waisted hysteresis loops: mineral magnetic characteristics and discrimination of components in mixed magnetic systems. Journal of Geophysical Research 100, 17,909–17,924.
Roberts, A.P., Wilson, G.S., Florindo, F., Sagnotti, L., Verosub, K.L., Harwood, D.M., 1998. Magnetostratigraphy of lower Miocene strata from the CRP-1 Core, McMurdo Sound, Ross Sea, Antarctica. Terra Antartica 5, 703–713.
Roberts, A.P., Wilson, G.S., Harwood, D.M., Verosub, K.L., 2003. Glaciation across the Oligocene–Miocene boundary in southern McMurdo Sound, Antarctica: new chronology from the CIROS-1 drill hole. Palaeogeography, Palaeoclimatology, Palaeoecology 198, 113–130.
Sagnotti, L., Florindo, F., Wilson, G.S., Roberts, A.P., Verosub, K.L., 1998. Environmental magnetism of lower Miocene strata from the CRP-1 core, McMurdo Sound, Antarctica. Terra Antartica 5, 661–667.
Sagnotti, L., Verosub, K.L., Roberts, A.P., Florindo, F., Wilson, G.S., 2001. Environmental magnetic record of the Eocene–Oligocene transition in the CRP-3 drillcore, Victoria Land Basin, Antarctica. Terra Antartica 8, 507–516.
Sagnotti, L., Roberts, A.P., Weaver, R., Verosub, K.L., Florindo, F., Wilson, G.S., Pike, C.R., Clayton, T., 2005. Apparent magnetic polarity reversals due to remagnetization resulting from late diagenetic growth of greigite from siderite. Geophysical Journal International 160, doi:10.1111/j.1365–246X.2004.02485.x.
Scherer, R.P., Bohaty, S.M., Harwood, D.M., 2000. Oligocene and lower Miocene siliceous microfossil biostratigraphy of Cape Roberts Project core CRP-2/2A, Victoria Land Basin, Antarctica. Terra Antartica 7, 417–442.
Verosub, K.L., Florindo, F., Sagnotti, L., Roberts, A.P., Wilson, G.S., 2000. Environmental magnetism of Oligocene–Miocene glaciomarine strata from the CRP-2/2A drillcore, Victoria Land Basin, Antarctica. Terra Antartica 7, 599–608.
Watkins, D.K., Villa, G., 2000. Palaeogene calcareous nannofossils from CRP-2/2A, Victoria Land Basin, Antarctica. Terra Antartica 7, 443–452.
Watkins, D.K., Wise Jr., S.W., Villa, G., 2001. Calcareous nannofossils from Cape Roberts Project drillhole CRP-3, Victoria Land Basin, Antarctica. Terra Antartica 8, 339–346.
Webb, P.-N., Wilson, G.S. (Eds.), 1995. The Cape Roberts Project—Antarctic stratigraphic drilling: Proceedings of the U.S. Planning Workshop, Report-Byrd Polar Research Center, vol. 10, 117 pp.
Wilch, T.I., Lux, D.R., Denton, G.H., McIntosh, W.C., 1993. Minimal Pliocene–Pleistocene uplift of the Dry Valleys sector of the Transantarctic Mountains: a key parameter in ice sheet reconstructions. Geology 21, 841–844.
Wilson, G.S., Roberts, A.P., Verosub, K.L., Florindo, F., Sagnotti, L., 1998. Magnetobiostratigraphic chronology of the Eocene–Oligocene transition in the CIROS-1 core, Victoria Land Margin, Antarctica: implications for Antarctic glacial history. Geological Society of America Bulletin 110, 35–47.
Wilson, G.S., Florindo, F., Sagnotti, L., Verosub, K.L., Roberts, A.P., 2000a. Magnetostratigraphy of Oligocene–Miocene glaciomarine strata from the CRP-2/2A core, McMurdo Sound, Ross Sea, Antarctica. Terra Antartica 7, 631–646.
Wilson, G.S., Bohaty, S.M., Fielding, C.R., Florindo, F., Hannah, M.J., Harwood, D.M., McIntosh, W.C., Naish, T.R., Roberts, A.P., Sagnotti, L., Scherer, R., Strong, C.P., Verosub, K.L., Villa, G., Watkins, D.K., Webb, P.-N., Woolfe, K.J., 2000b. Chronostratigraphy of CRP-2/2A, Victoria Land Basin, Antarctica. Terra Antartica 7, 647–654.
Wilson, G.S., Lavelle, M., McIntosh, W.C., Roberts, A.P., Harwood, D.M., Watkins, D.K., Villa, G., Bohaty, S.M., Fielding, C.R., Florindo, F., Sagnotti, L., Naish, T.R., Scherer, R.P., Verosub, K.L., 2002. Integrated chronostratigraphic calibration of the Oligocene–Miocene boundary at 24.0$\pm$0.1 Ma from the CRP-2A drill core, Ross Sea, Antarctica. Geology 30, 1043–1046.
Wrenn, J.H., Hart, G.F., 1988. Paleogene dinoflagellate cyst biostratigraphy of Seymore Island, Antarctica. In: Feldman, R.M., Woodburn, M.O. (Eds.), Geology and Paleontology of Seymore Island, Antarctic Peninsula, Geological Society of America Memoir, vol. 169, pp. 321–447.
Zachos, J., Pagani, M., Sloan, L., Thomas, E., Billups, K., 2001. Trends, rhythms, and aberrations in global climate 65 Ma to present. Science 292, 686–693.